DOI: 10.21062/mft.2021.081 http://www.journalmt.com

Improving Rotary Draw Bending Process by Changing a Geometry of the Pressure Die

Jan Řiháček (0000-0003-2669-2730), Eva Peterková (0000-0001-6648-6793), Michaela Císařová (0000-0001-7568-7378)
Brno University of Technology, Faculty of Mechanical Engineering, Institute of Manufacturing Technology, Technická 2896/2, 616 69 Brno, Czech Republic, E-mail: rihacek.j@fme.vutbr.cz

The paper is focused on an analysis and optimization of the rotary draw bending process to eliminate bent tube ovality by modification of the pressure die geometry. The bending process is realized on Wafios CNC bending machine. A tube that is bent for an automotive application is made of 34MnB5 steel. Currently, after tube bending process by an angle of 120°, an unacceptable ovality occurs. Therefore, it is necessary to improve the quality of production and thus prevent the formation of unacceptable ovality. In this case, the optimization of the pressure die geometry is carried out. For this reason, a numerical simulation using finite element method in ANSYS software is performed. Before the actual optimization, an accuracy of the simulation is verified by analysing of the current state and comparing it with simulation results.

Keywords: FEM, numerical simulation, ANSYS, 34MnB5 steel, tube bending

1 Introduction

An area of tube bending is currently widely used and discussed mainly due to a trend of reducing the weight of parts and the use of ever newer and stronger materials, not only in the automotive industry. Bending is the primary technology of sheet metal forming, through which the desired shape of tubular parts, profiles, bars or sheets is achieved. [1], [2]

One of the most common tube bending methods is, so called, rotary draw bending (RDB). Tubes with a diameter up to 250 mm are usually bent to a bending angle of up to 180° by mentioned method. In this case, the bending process is realized by rotating bend die, to which the tube is attached by means of a clamp die. During the bending operation, the pressure die forces the tube into the groove of the bend die, so it can be formed correctly, see Fig. 1. [3]

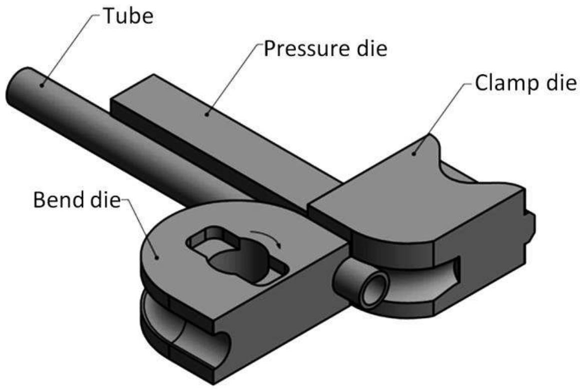

Fig. 1 *Basic principle of RDB*

The pressure die can be firmly fixed in place during the forming process or move alongside with the bent tube. The movement of the pressure die alongside the tube can be also describe as boosting. The movable pressure die provides better guidance and eliminates wear on the contact surfaces against the fixed die. It is important to note, that RDB dominates the tube bending landscape. RDB has gained more applications in automotive industries or aerospace thanks to its wide possibilities. [3], [4]

The main technological problem in the tube bending lies in forming of the hollow part, which increases the problems in the form of defects. The occurrence of defects is an inevitable phenomenon in practice. Defects are often caused by non-compliance with technological parameters. Geometric parameters, material, chosen technology, used tools and their wear play an important role in the bending practice. However, many defects are concomitant bending effect and they cannot always be eliminated. Nevertheless, there are certain actions that reduce the defects rate to a tolerated level. The most common defects in the tube bending process are:

- cross-section flattening – ovality,
- wall thinning,
- wall wrinkling,
- enormous springback.

1.1 Tube Ovality

The ovality is one of the basic defects in which the tube cross-section is flattened. Due to the force effects, the originally circular cross-section deforms into complex shapes, often compared to an ellipse, as can be seen in Fig. 2.

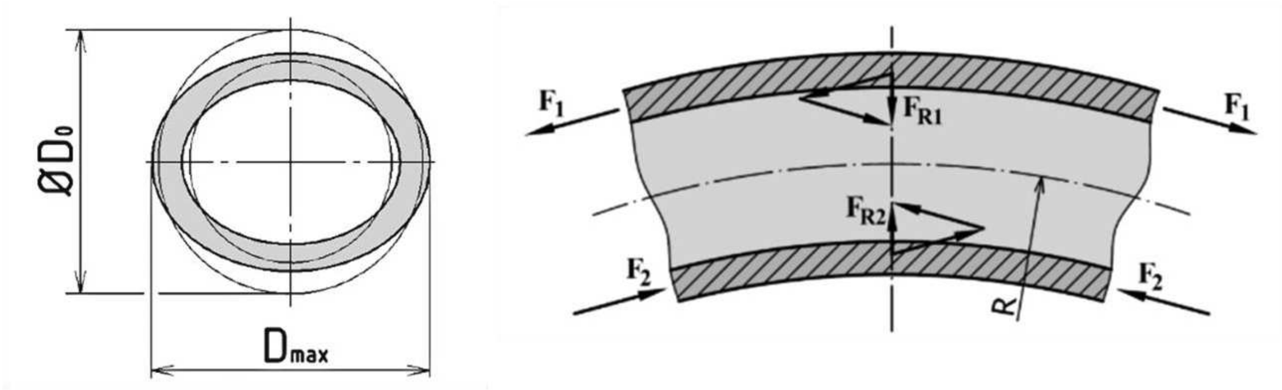

Fig. 2 *Force decomposition at the bending point and cross-section ovality [4]*

There are several relationships to describe this deformation. The calculation of the ovality coefficient is often defined by manufacturing companies or their customers, as well as in the case of ovality allowable values. Equation (1) gives one of the possible calculations of the ovality coefficient:

$$K_O = \frac{D_{max} - D_{min}}{D_0} \cdot 100 \qquad (1)$$

Where:
K_O........the ovality coefficient [%],
D_{max}......the maximum cross-sectional dimension [mm],
D_{min}......the minimum cross-sectional dimension [mm],
D_0.........the initial tube diameter [mm].

The ovality origin can be explained by the decomposition of internal forces, assuming neglecting the influence of pressure from the supporting tools that contribute to the formation of ovality. The bending moment induces tensile and compressive axial stresses on the outer and inner side of the bent tube caused by the internal forces F_1 and F_2, as it is clearly shown in Fig. 2. This force action leads to radial forces F_{R1} and F_{R2} which cause the ovality. It is accompanied by the transfer of material, which results in thinning of the wall on the outer radius and widening in the pressure area. This change in cross-section increases the stress in the material. It follows that the radial forces causing ovality also increase while increasing the bending angle.

As it was experimentally found, e.g. in [5], the ovality is not uniform in the longitudinal tube direction, as can be seen in Fig. 3. The bent tube can be divided into 3 parts depending on the bending angle. Uniform oval area "A", uneven oval area "B" and undeformed area "C". The unevenly deformed area can be explained by the action of forces from the tools at the ends of the tube [6]. Closer to the centre of the bend, these forces are already negligible, according to the Sant-Venant principle. In the area "A", only the bending moment acts. Therefore, a constant ovality of larger values can be expected than in area "B" [7].

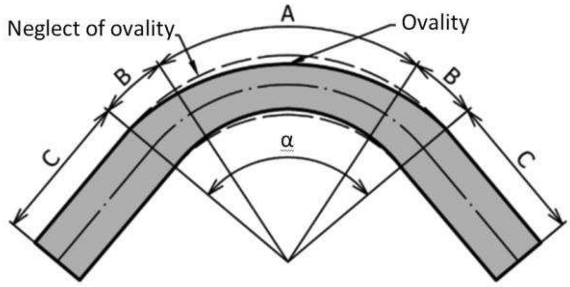

Fig. 3 *Uneven distribution of ovality [4]*

In the manufacturing process, there is usually efforts to avoid ovality. In the following text, some possible ways to influence or reduce the ovality will be presented:

- Axial compressive force – one of the possibilities leading to reduce the ovality is the additional pressure action on the tube. Axial pressure force pushes more material into a focal point of deformation. This acting reduces the proportion of tensile stress at a critical point. Article [8] demonstrates the positive effects on the process. The influence of the compressive force reduces the ovality coefficient and at the same time reduces the wall thinning on the outer radius of the tube.
- Fillers – another way to reduce the ovality is to use fillers that provide necessary support for the tube cross-section during the bending operation. Currently, liquid, rigid, powdery or mechanical fillings (e.g. densely coiled springs, polyurethane rollers, nylon flexible

inserts or metal stabilizing mandrels) can be used.

- Modification of the tool geometry – the functional surfaces of tools that come into contact with the tube and have the greatest influence on the resulting bending quality are the grooves of the bend or pressure die. The shape of grooves represents the negative of the bent blank. In the case of bar or tube bending, the groove copies a circular shape in most cases. However, when using grooves that do not exactly copy the shape of the tube, an uneven force is applied to the bent part, which can reduce the ovality in some cases. Many authors have dealt with the phenomenon of the tool modification in the past, e.g. [3], [4] or [9]. This approach represents a potential for improvement, which is not so much used in practice yet.

2 Investigated Problem

The investigated semi-finished product for experimental tests is a cold-drawn tube, which is made of 34MnB5 high-strength steel. As the designation suggests, the steel is low-alloyed with boron, manganese and is excellently weldable due to its low carbon content. Basic chemical composition and mechanical properties according to tensile test results are summarized in Tab. 1 and Tab. 2.

***Tab. 1** Mechanical properties of 34MnB5 steel [4]*

Yield stress	R_e	[MPa]	350
Ultimate strength	R_m	[MPa]	619
Young's modulus	E	[GPa]	191
Ductility	A_5	[%]	12.5

***Tab. 2** Chemical composition of 34MnB5 steel [4]*

%C	%Mn	%Si	%P	%S
0.33-0.37	1.2-1.4	0.15-0.30	max. 0.02	max. 0.005
%Al	%Ti	%Cr	%B	%Cu
0.02-0.05	0.02-0.05	0.10-0.18	0.0015-0.0035	max. 0.1

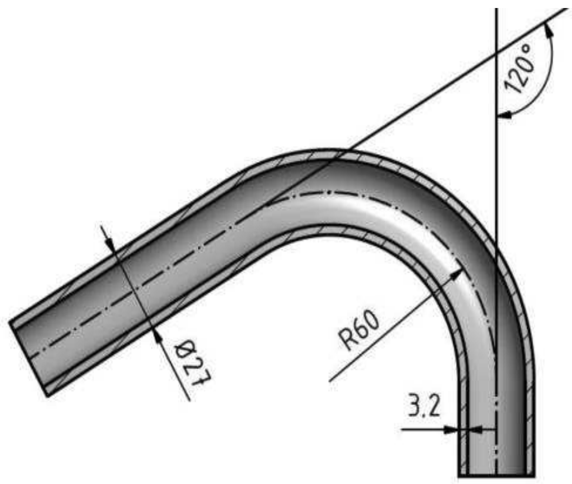

***Fig. 4** Required bend shape*

The requirement is to bend the tube with a diameter of 27 mm and a wall thickness of 3.2 mm by an angle of 120°. In this case, a bending radius is 60 mm, see Fig. 4.

The bending of tube to required angle was performed on Wafios RBV 60 ST CNC bending machine. The basic technical parameters of the machine are summarized in Tab. 3.

The bending die rotated about the central bending axis with an angular velocity of 40°·s^{-1}. Guided end of the tube and the pressure die move in a straight line in the axial direction with a length of 120.69 mm. A 1 500 mm long tube was used for the experiments. According to the possibilities of the machine, the test shape of the specimen was designed so that the semi-finished product was used to the maximum, but without a collision with the machine, see Fig. 5. In this case, 6 identical bends were made on each test tube.

***Tab. 3** Basic technical data of Wafios RBV 60 ST CNC bending machine [4]*

Bending capacity		Maximal bending geometry parameters		Maximal speeds	
Bending torque	8 kNm	Tube diameter	35 mm	Advance feed	1 700 mm·s^{-1}
Clamping force	140 kN	Feed length	3 500 mm	Rotation	450°·s^{-1}
Boost pressure	50 kN	Bending angle	195°	Bending	180°·s^{-1}

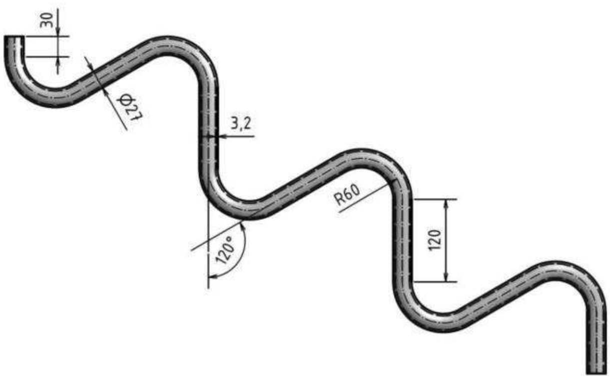

Fig. 5 *The specimen geometry*

The bent cross-section is analysed after a bending angle step of 20° (see Fig. 6) by using SSM-3E stereo microscope equipped with USB camera. In individual places, sections were made and changes in the ovality and minimum thickness were monitored. To refine the results, measurements were repeated and the ovality was averaged from up to 15 bends in one place.

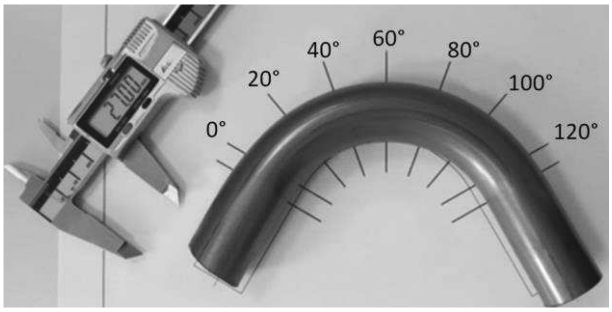

Fig. 6 *The ovality measurement*

The evaluation of the ovality according to equation (1) was performed. Detected course of the ovality coefficient depending on the bending angle is shown in Graph 1. In the graph, an uneven course of ovality can be observed, the value of which is on average around 5.4 %. The highest value was found for an angle of 100°, namely 6.13 %. At this point, the cross-section changes in the radial direction to the axis of rotation from the original 27 mm to 25.32 mm. The value measured in the axial direction to the direction of rotation is almost unchanged (27.07 mm).

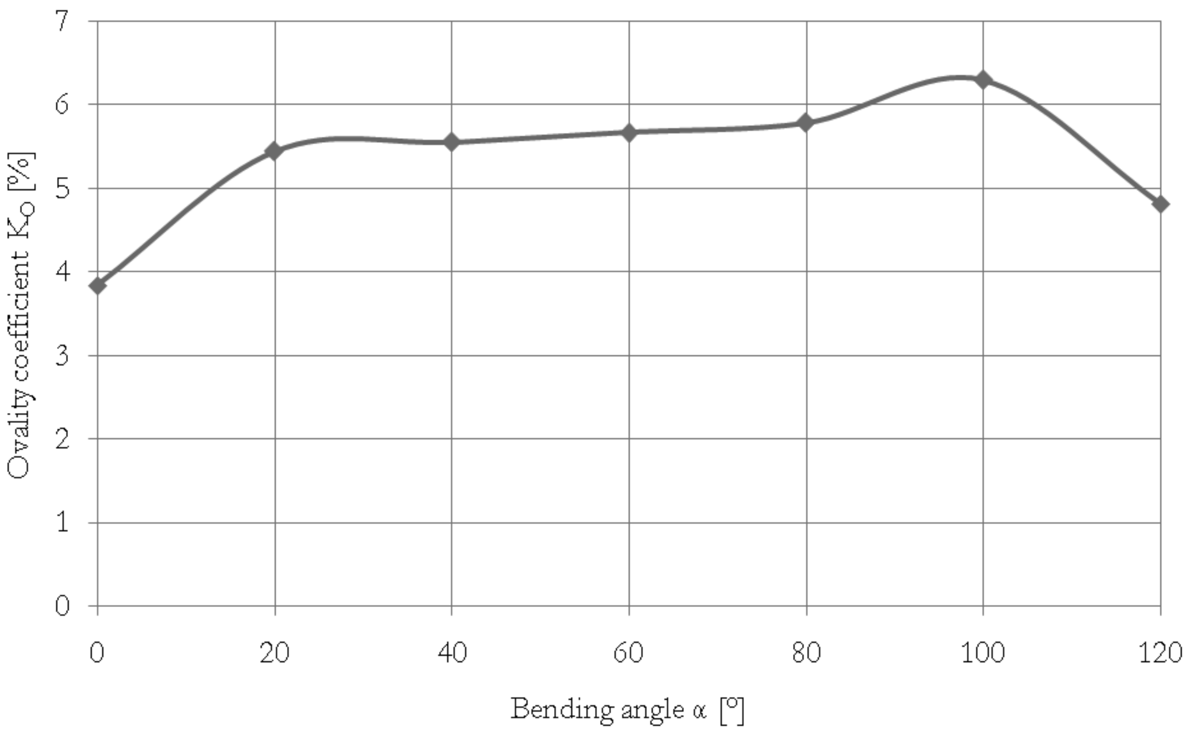

Graph 1 *Detected change in the ovality*

Graph 2 shows the change in the detected minimal wall thickness of the bent tube, which corresponds to the detected ovality. The minimum thickness for the section in 100° cut is 2.88 mm, which is a 10 % decrease from the original thickness. In the rest of the most exposed section (20° to 100°), the thickness value is already kept at approx. 2.9 mm.

In an effort to improve the ovality, a numerical analysis of the bending process is used in the following. Even before the actual optimization, it is necessary to verify the correctness and accuracy of the theoretical model by comparative simulation of the current state.

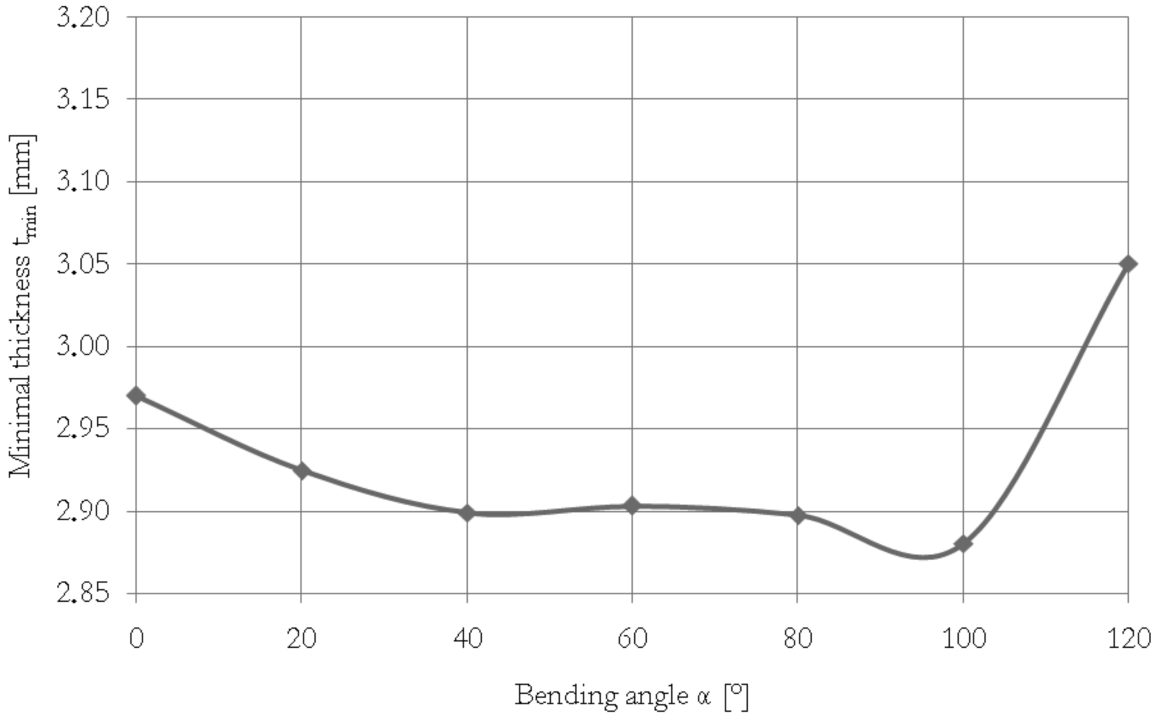

***Graph 2** Detected change in the minimal thickness*

3 Numerical Simulation

For this purpose, the numerical simulation using finite element method (FEM) in ANSYS Workbench software was used. Firstly, a material model was determined. Graph 3 shows the hardening curve plot according to tensile test results for temperature of 25 °C and mean value of strain rate of 0.01 s^{-1}. Elastic properties were set based on the values from Tab. 1. [10], [11]

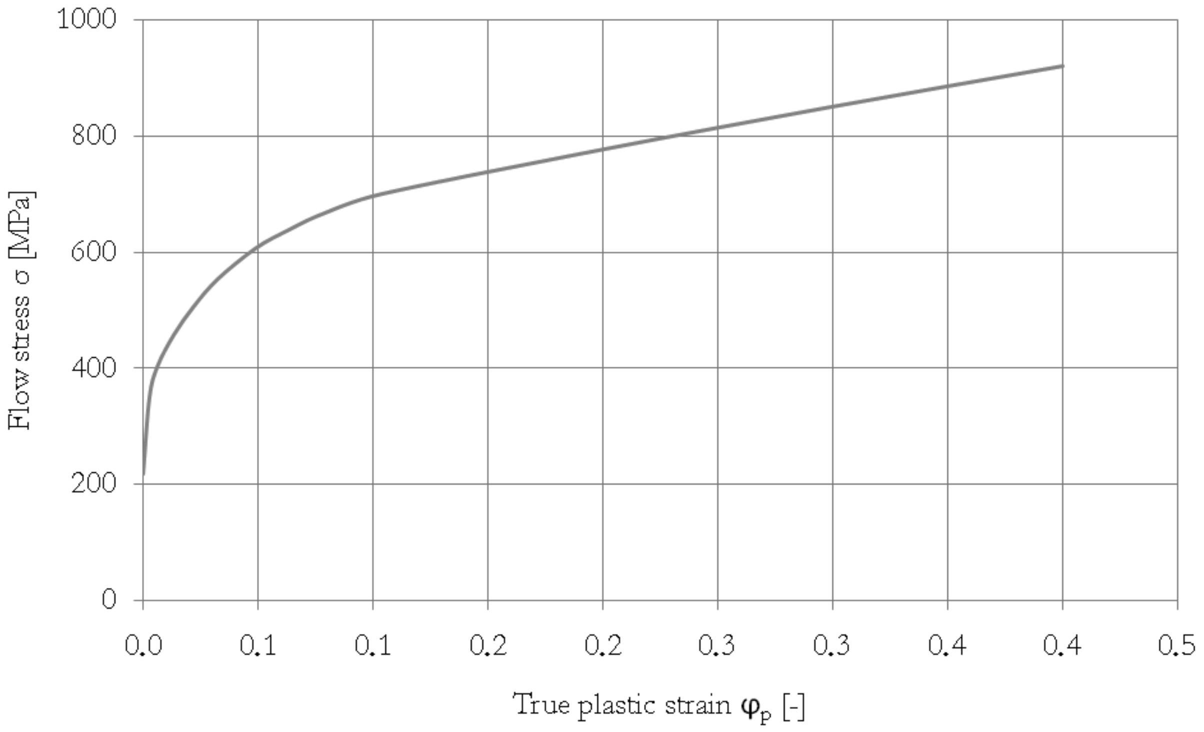

***Graph 3** Flow stress of 34MnB5 steel*

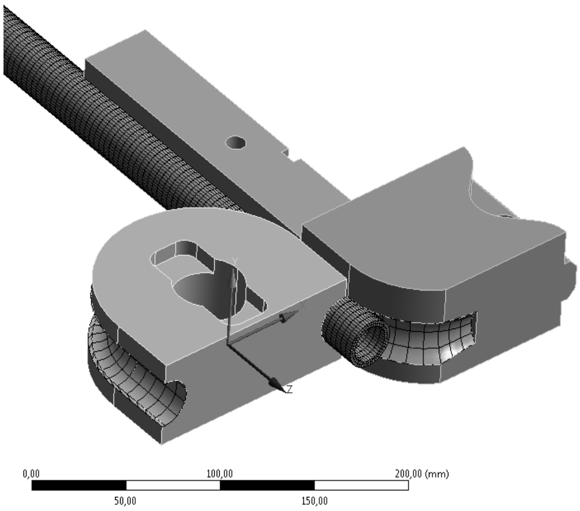

Fig. 7 *The FEM geometric model for rotary draw bending*

All tools were further considered as ideally rigid. Therefore, only contact elements were used. For friction description, the Coulomb's coefficient of friction was set to 0.15. The discretized simulation model is shown in Fig. 7. The lateral pressure of the clamping die and the pressure die on the tube was originally set by a force. However, the force effect fluctuates depending on the resistances during the process in real manufacturing process. For better stability of simulation and better interpretation of results, the tools movement is controlled only by their position. [12]

After the calculation, it is possible in post-processing to focus on simulation results for the verification of the simulation. Firstly, the experimentally determined ovality curves and the minimal wall thickness of the tube were compared, see Graph 4 and Graph 5.

In this regard, the results show a fairly good agreement between experimentally measured and calculated data. However, at the edges of the monitored area, there are significant fluctuations in the comparison of the monitored values. This can be caused by simplified boundary conditions of the FEM simulation, which were used to stabilize and speed up the calculation.

Another possibility to verify the numerical simulation is to compare the geometry of the deformed cross-section of the tube. Fig. 8 shows a comparison of the mentioned geometry in a section at an angle of 20°, i.e. in the most problematic place in terms of ovality and thinning.

As can be seen from Fig. 8, the geometry predicted by the simulation is close to the experimentally determined contour with a deviation not exceeding 0.62 mm. It is possible to note that the simulation with its results almost coincides with real state and it is therefore possible to use it in the following for optimization.

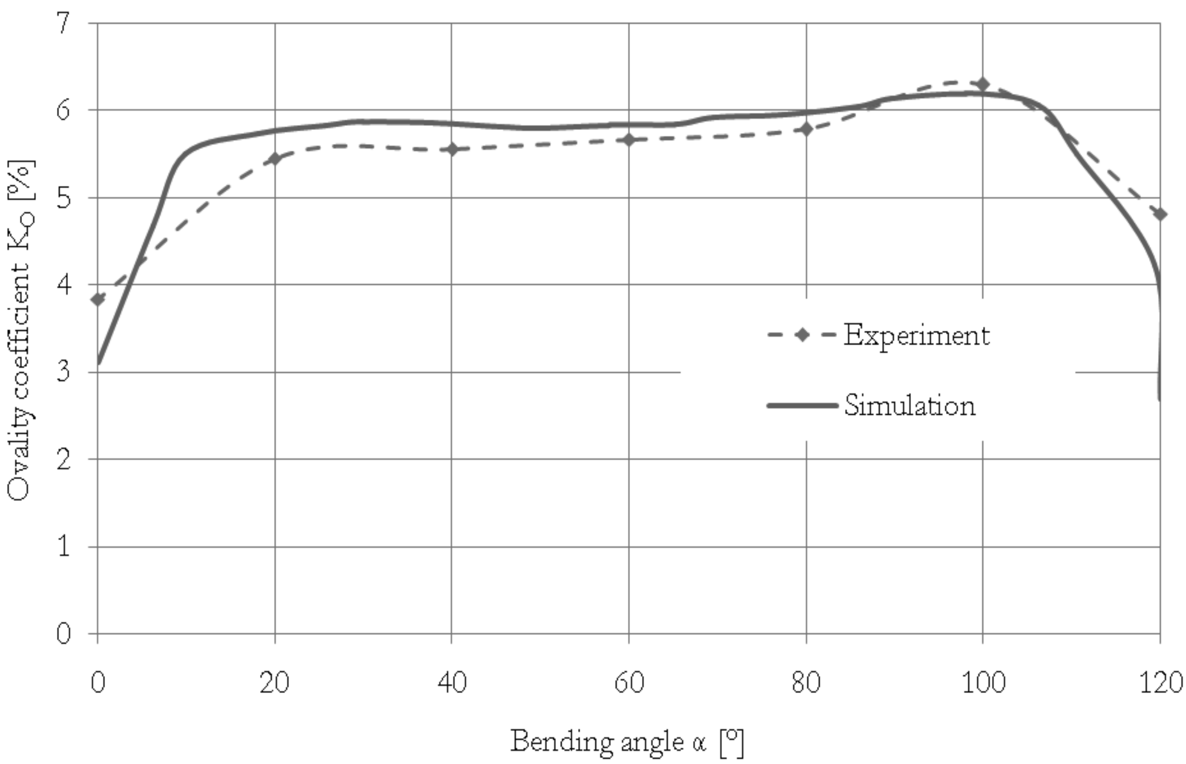

Graph 4 *Comparison of change in the ovality*

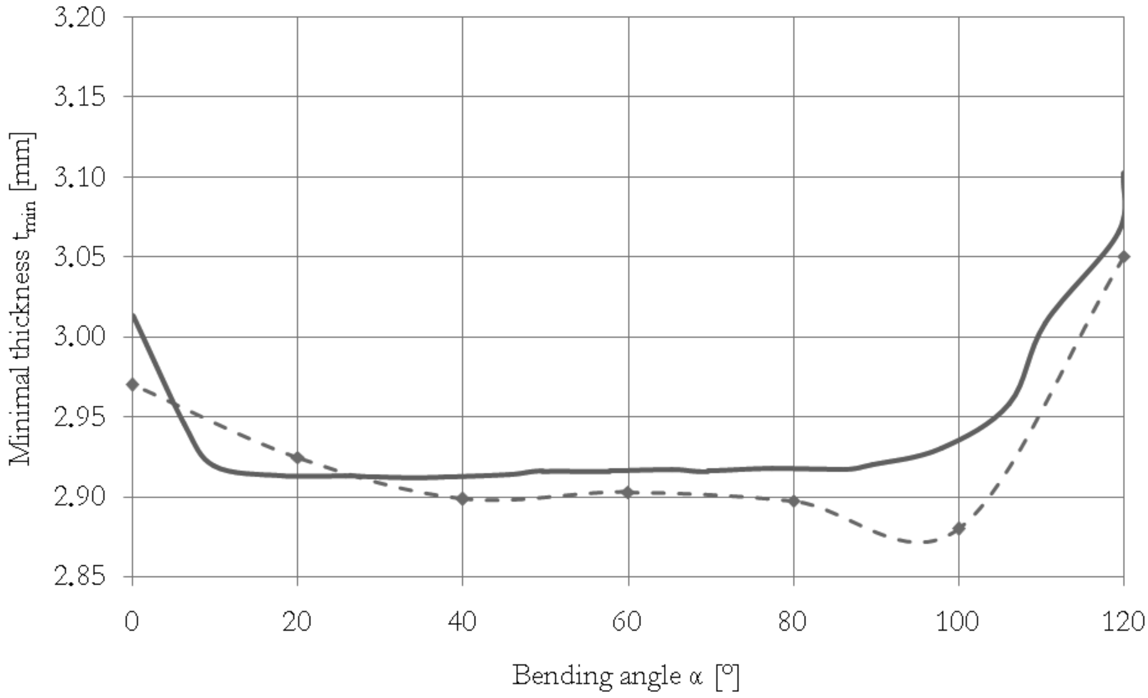

Graph 5 *Comparison of change in minimal thickness*

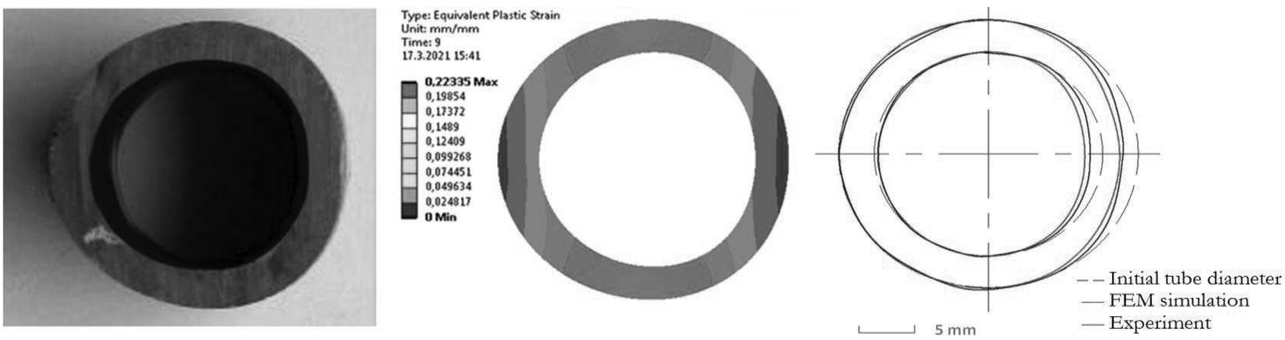

a) specimen cross-section *b) results of FEM simulation* *c) comparison of contours*

Fig. 8 *Comparison of the deformed cross-section geometry*

4 Optimization of the Pressure Die Geometry

In an effort to interfere as little as possible in the production process, an optimized tool geometry was designed that only involves changing the shape of the pressure die groove. The new design of the pressure die groove no longer completely copies the formed tube, but adheres to it only at two points (shape A) or three points (shape B). In this case, the cross-section of the groove has the shapes according to Fig. 9. However, the groove connects tangentially the bent tube. Within the bending optimization, a variation of the groove angle θ = 20° to 100° was considered for both analysed variants.

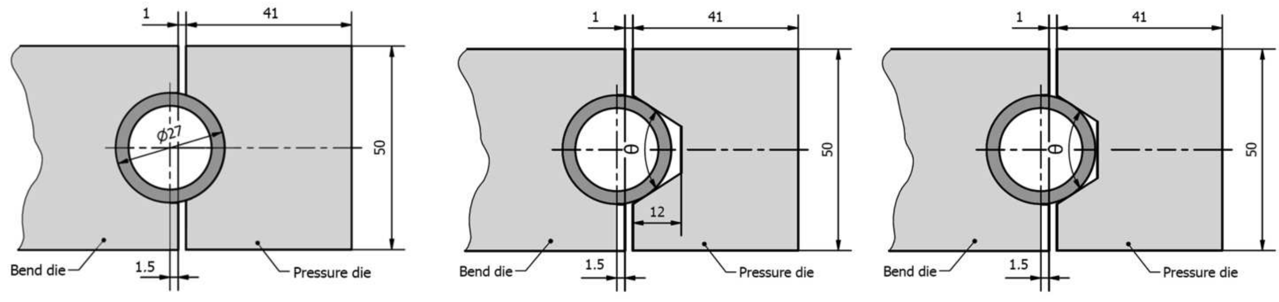

a) initial unmodified geometry *b) optimized shape A* *c) optimized shape B*

Fig. 9 *Optimized pressure die geometry*

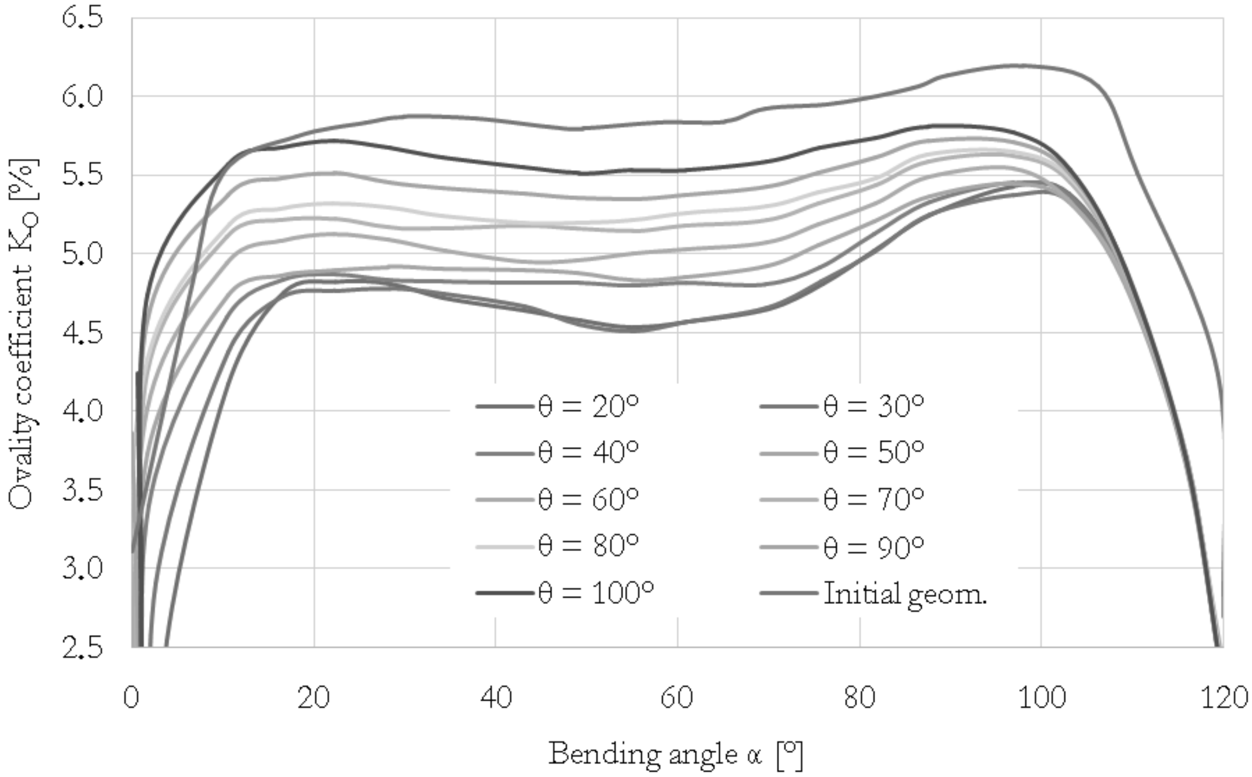

Graph 6 *Change in the ovality for optimised A*

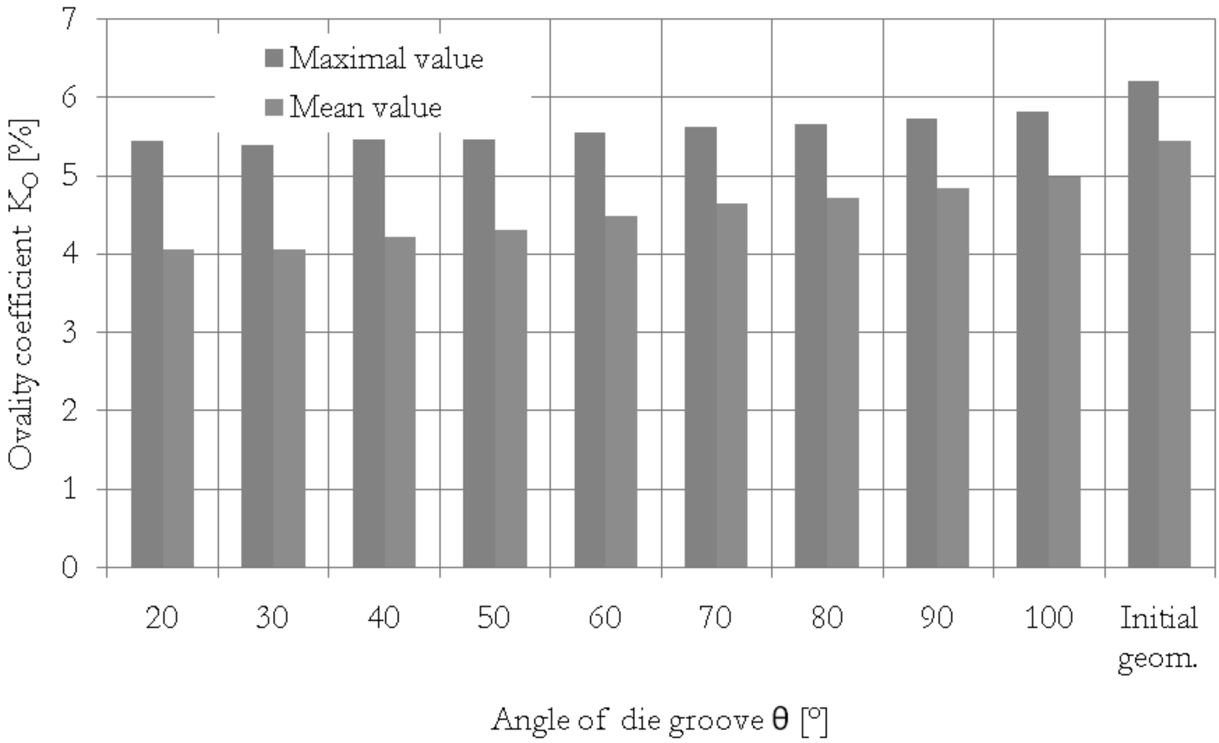

Graph 7 *Maximal and mean values of the ovality coefficient for optimised A*

In the case of shape A, the results of performed numerical simulations, which summarize the change in the ovality coefficient, are shown in Graph 6 and Graph 7. From the point of view of comparison with the current state, it is clearly evident that all variants achieve better results than the initial geometry of the pressure die. If the value of the ovality coefficient is compared across the individual variants of θ angle, the achieved maximum values differ from each other by up to 7.6 %. Higher θ angles are characterized by more flattened curve of the change in the ovality coefficient, but also by the overall higher achieved ovality, which does not differ much from the initial geometry. In contrast, lower values of θ angle help to prevent the ovality formation more, although in this case it is possible to observe larger fluctuations between the minimum and maximum ovality in the monitored area. The best results are achieved by the modified geometry of the pressure die with an angle θ = 30°, which reaches an improvement of 13 % when comparing the maximum achieved values. Similarly, the average values of the ovality coefficient can be compared. Here, the improvement in the ovality coefficient reaches up to 25 %. For lower angles, the ovality coefficient increases slightly.

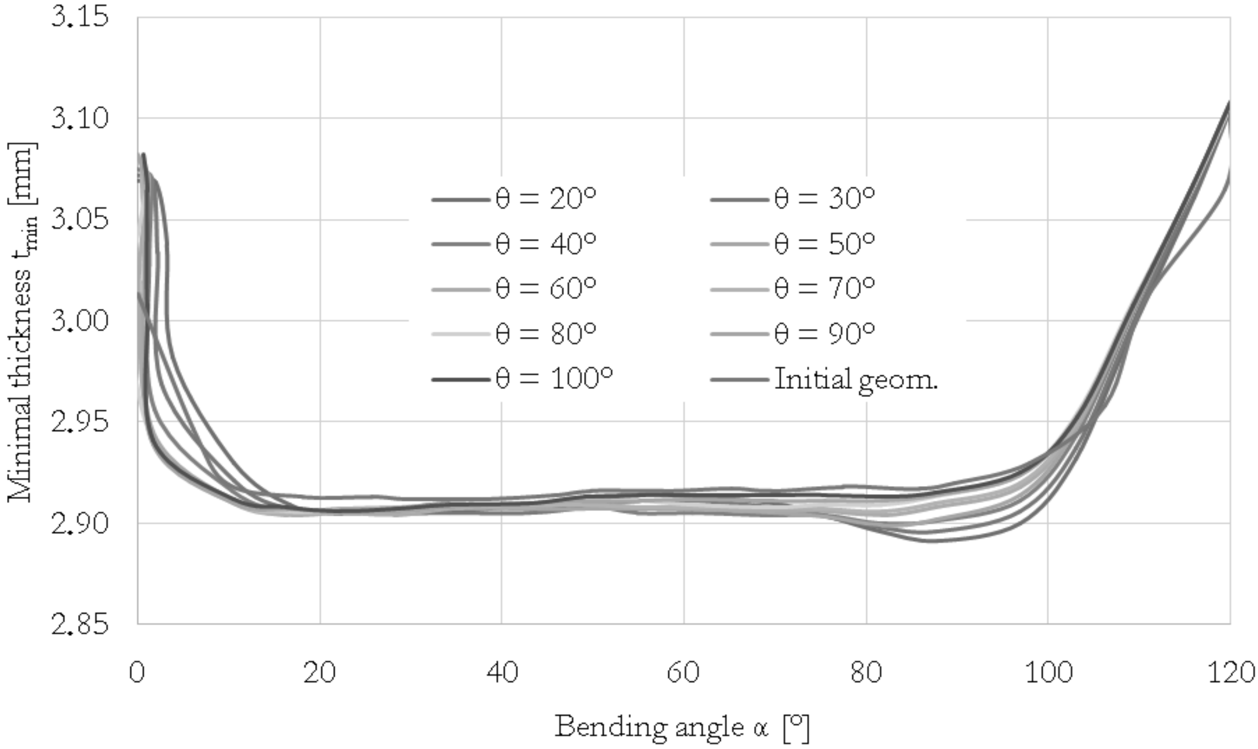

***Graph 8** Change in the wall thickness for shape A*

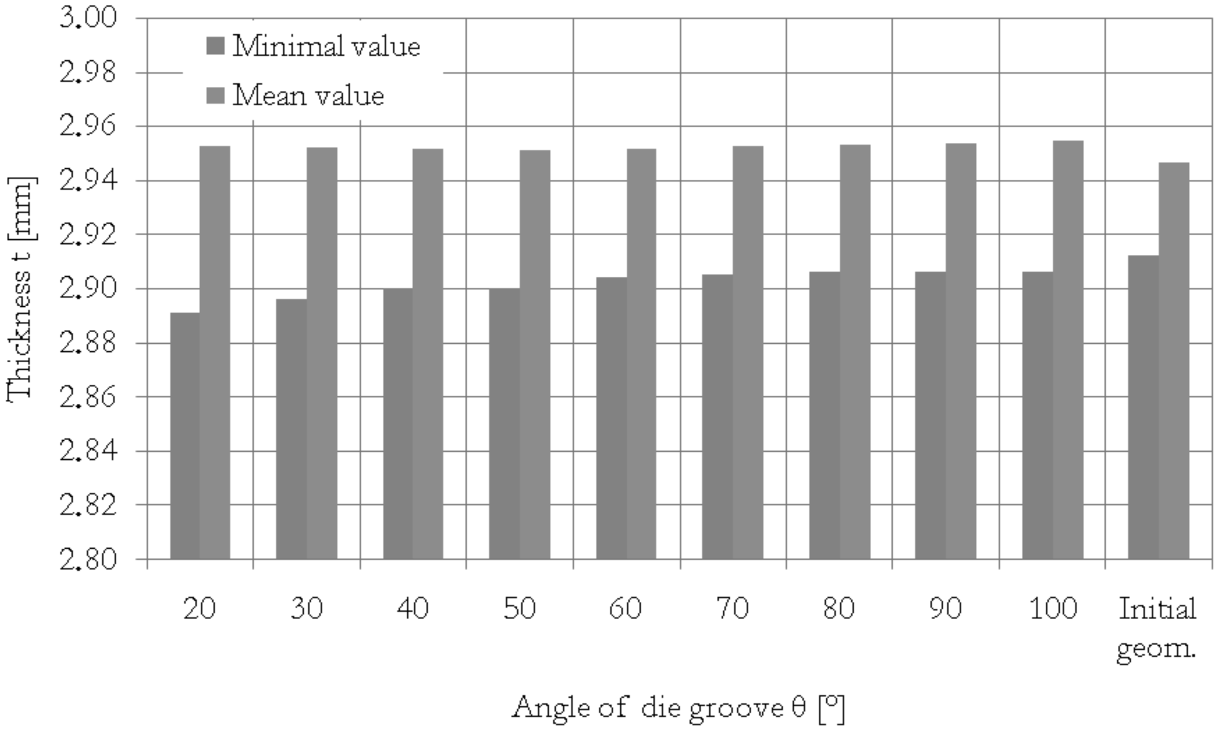

***Graph 9** Maximal and mean values of the thickness for shape A*

The change in the ovality corresponds to the change in the wall thickness of the bent tube, see Graph 8 and Graph 9. It is important to note, that in the variant which shows the greatest shift in the improvement of the ovality (θ = 30°), the greatest thinning of the cross-section occurs. Values of the minimum thicknesses differ only slightly for the individual investigated variants, in the order of 0.5 %, as it is clearly evident from the comparison in Fig. 14. However, in terms of comparison with the initial state, the tube thins more, by 0.55 % for θ = 30°. In the case of the mentioned variant, the total thinning is around 9.5 %.

The same can be done when evaluating the shape B. Comparison of the determined curves of the ovality coefficient change for the considered geometries of the pressure die with the angle θ = 20° to 100° again. Nevertheless, in the shape B, there is a three-point contact between the die and the tube during bending process (Fig. 9c). This modification means a different stress state, which in turn leads to differences in the detected ovality. As can be seen from results in Graph 10 and Graph 11, the modification of the geometry of the pressure die according to the B-shape leads to a certain improvement in ovality, but it certainly does not achieve the A-shape effect.

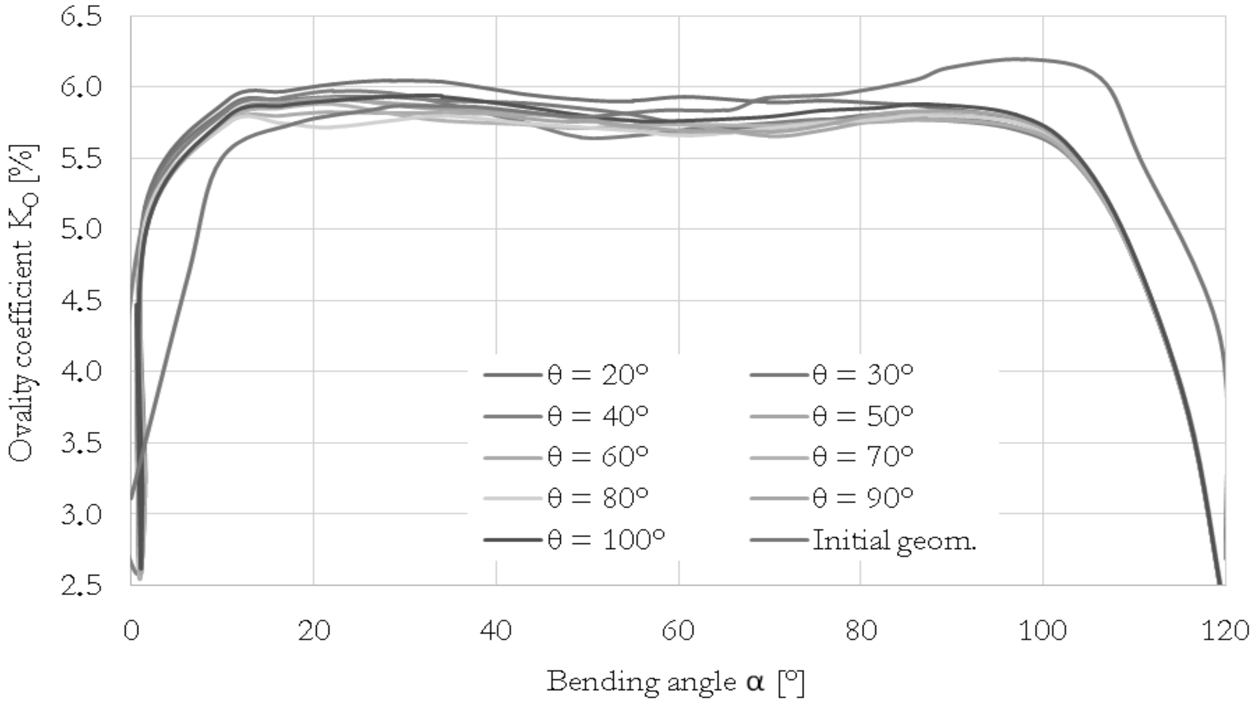

Graph 10 *Change in the ovality for shape B*

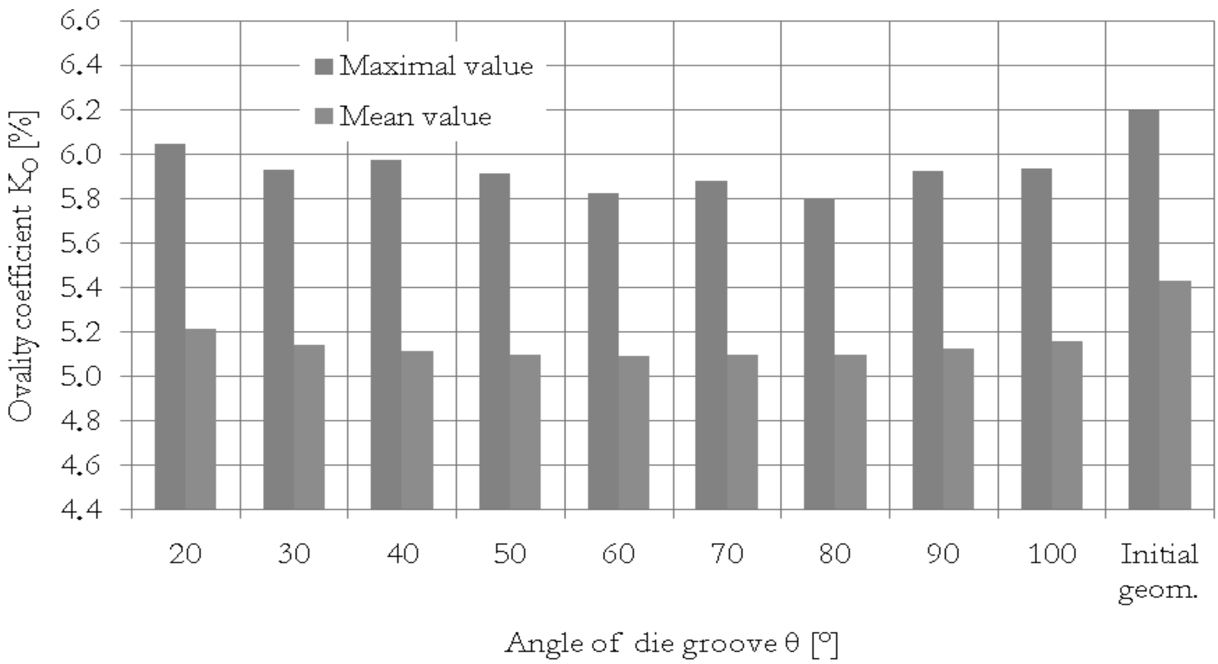

Graph 11 *Maximal and mean values of the ovality coefficient for shape B*

The best results in this respect are achieved by the variant with the angle θ = 80°, where the improvement in the maximal ovality coefficient reaches 6.3 % in comparison with the initial geometry. Some results, such as θ = 20°, even cause a higher ovality than the original unmodified geometry at a bending point around α = 20°. Of course, the achieved ovality will also affect the change in the wall thickness of the tube. Results of this analysis are shown in Graph 12 and Graph 13.

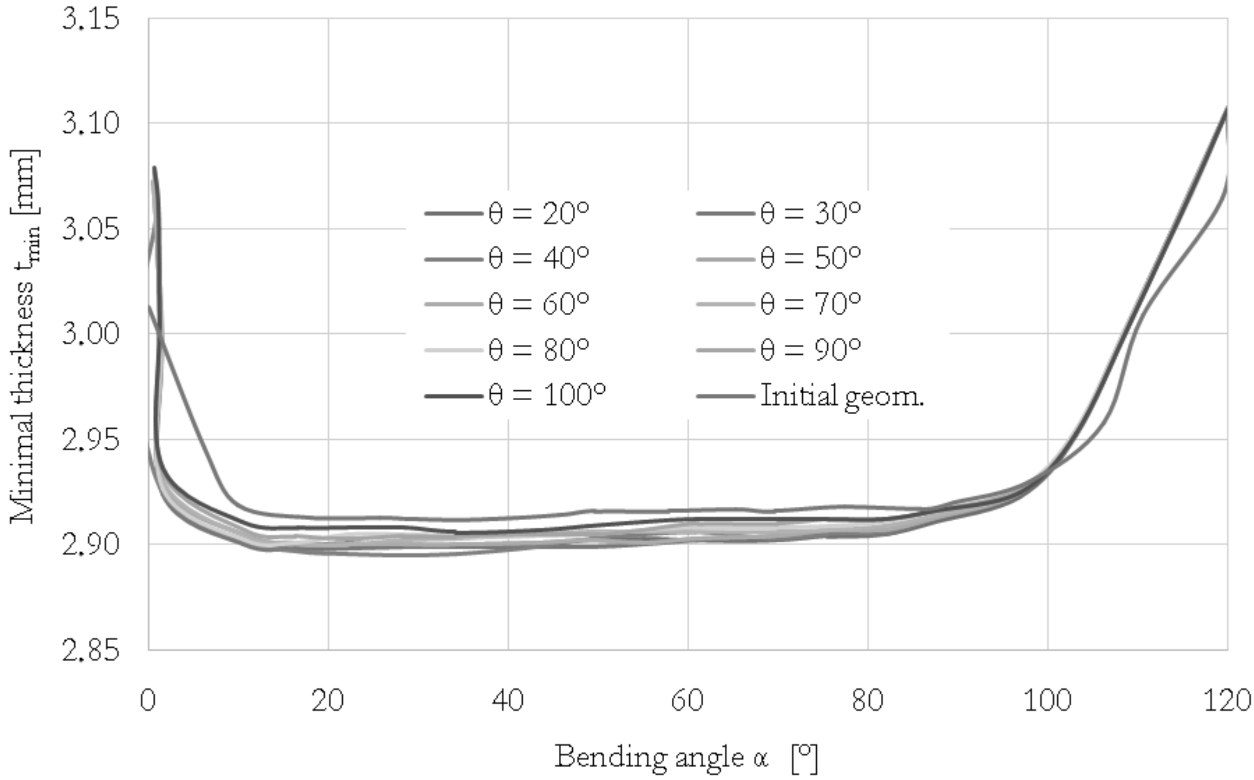

Graph 12 *Change in the wall thickness for shape B*

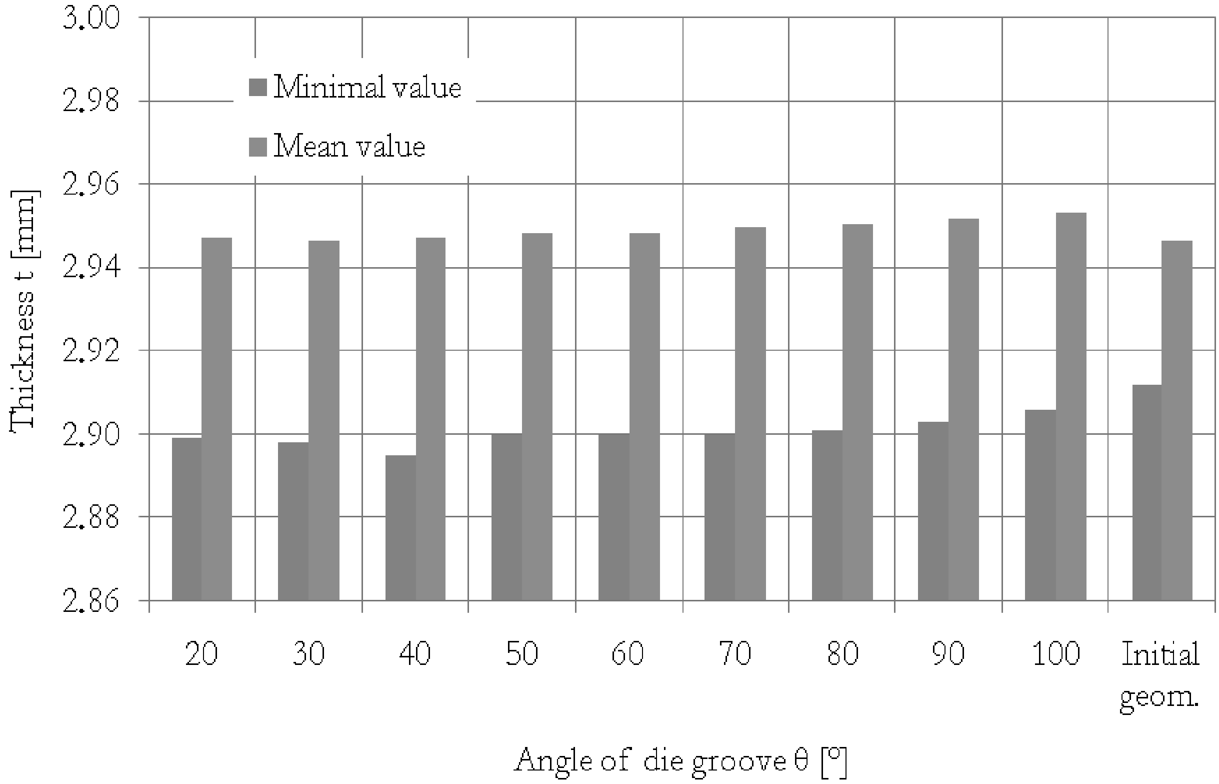

Graph 13 *Maximal and mean values of the thickness for shape B*

The distribution of the determined minimal and men thickness value is almost identical for all considered θ angles, i.e. approx. 2.9 mm as the minimal wall thickness (0.34% change from initial state) and approx. 2,95 mm (0.2% change from initial state towards less thinning).

5 Results and Discussion

If the above mentioned modifications of the pressure die groove geometry are compared, in terms of the achieved ovality and the change in the wall thickness, it is evident that the two-point contact between the tool and the tube is much more effective than the three-point contact, as can be seen from the above comparison. In the first step, the achieved improvement in detected maximal ovality coefficient was compared for all investigated cases, see Graph 14.

The comparison shows a significant difference between two optimized geometries. As it was mentioned before, the largest improvement in ovality value was detected when considering a die angle θ = 30°. For this modification, the improvement of ovality in the whole examined range of α is further summarized in Tab. 4.

Tab. 4 *Improvement of the ovality coefficient (Shape A, θ = 30°)*

	Ovality coefficient K_O [%]		
Angle α [°]	Initial geometry	Shape A	Improvement
0	3.115	3.072	1.380
20	5.780	4.760	17.647
40	5.837	4.690	19.651
60	5.837	4.570	21.706
80	5.986	4.950	17.307
100	6.180	5.330	13.754
120	2.693	2.233	17.081

The deformed cross-section of the bent tube for the best variant of the pressure die geometry (θ = 30°) is shown in Fig. 10. In addition to the deformed cross-section, the figure also shows the distribution of plastic deformation along the cross-section in individual sections corresponding to the angle α = 0° to 120°. It is clear that the largest deformation occurs on the sides of the bent cross-section, in the range α =20° to 100°.

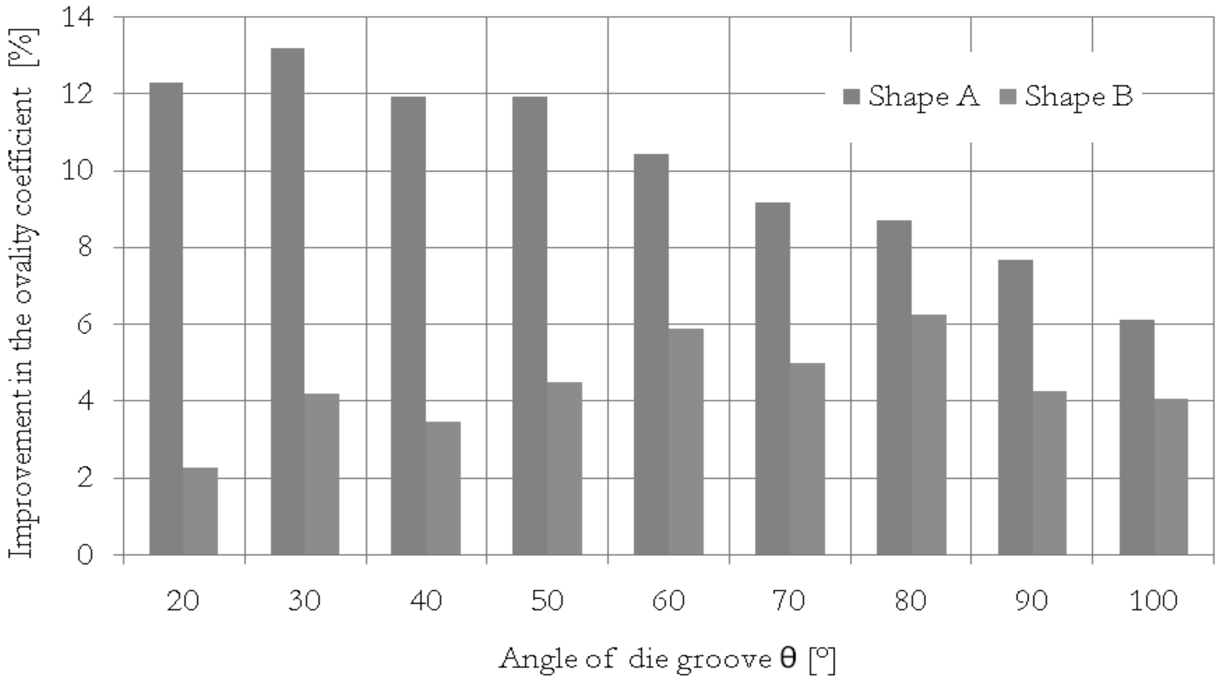

Graph 14 *Improvement of detected maximal ovality coefficient for both shapes*

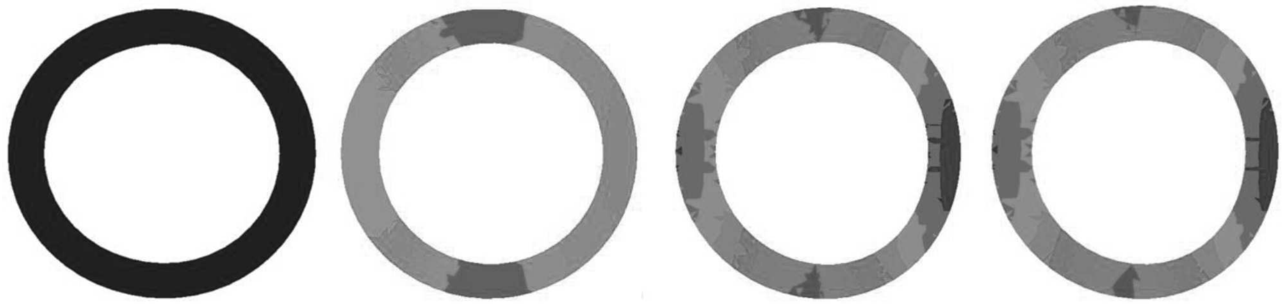

a) undeformed end of the tube *b) α = 0°* *c) α = 20°* *d) α = 40°*

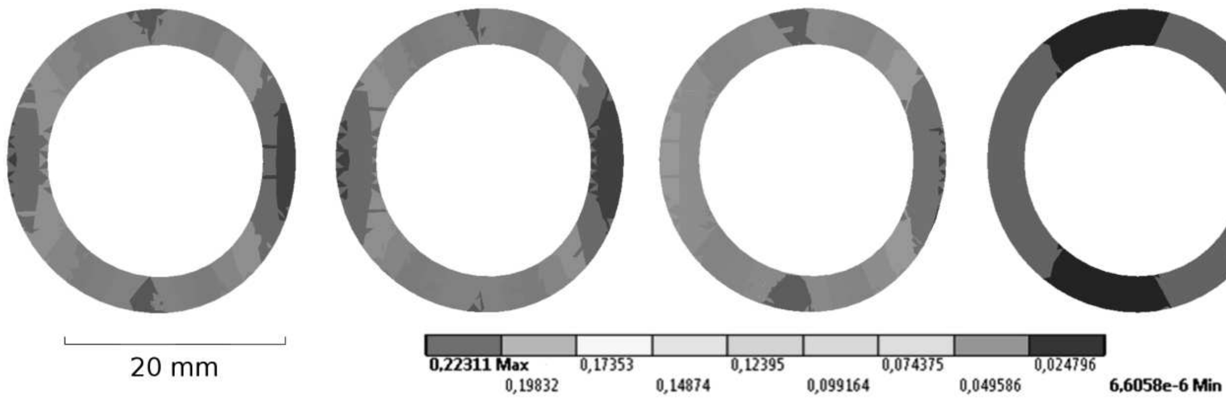

e) α = 60° *f) α = 80°* *g) α = 100°* *h) α = 120°*

Fig. 10 *Distribution of plastic strain on deformed cross-section geometry*

In the case of a comparison of the achieved minimal wall thickness, which to some extent corresponds to the ovality values, it can be stated that even in this area, shape A achieves better results than shape B. The overall comparison is provided by graph in Graph 15, which shows percentage change in the minimal detected thickness compared to the initial state without tool modification.

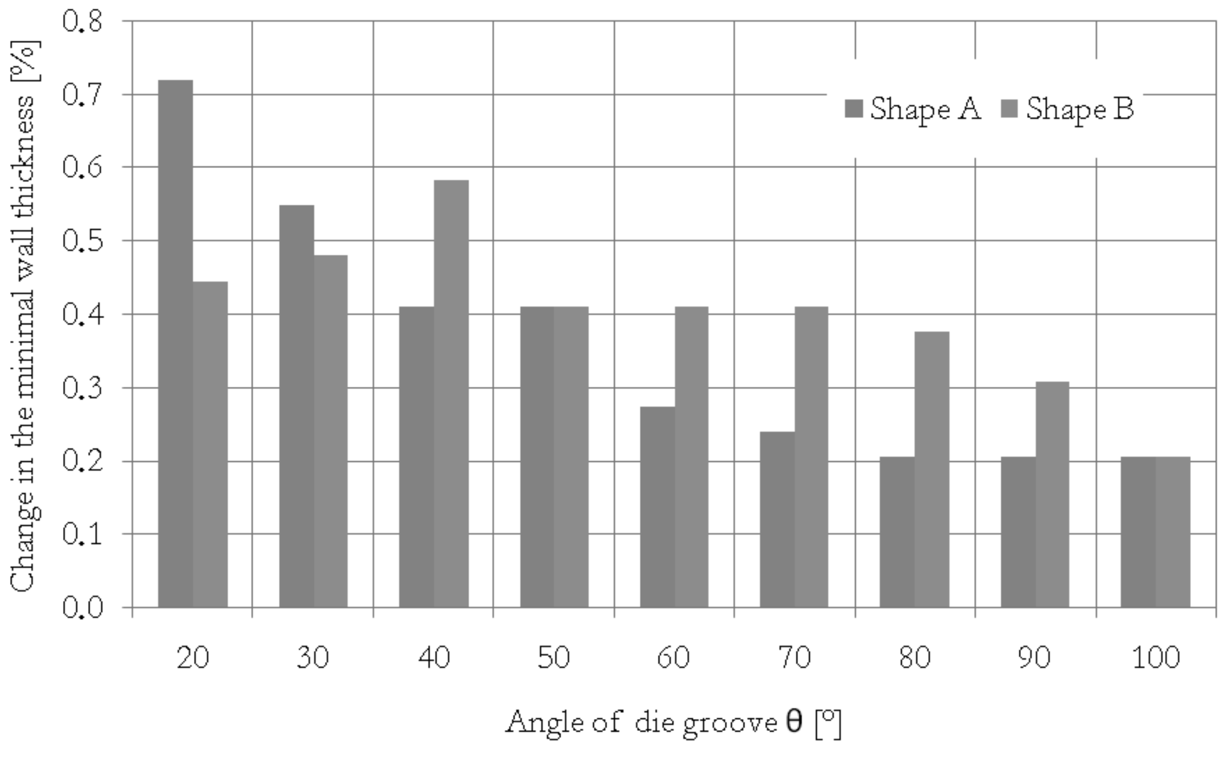

Graph 15 *Changes in detected minimal wall thickness for both shapes*

From this point of view, variants with a tool angle θ = 100° seem to be the most suitable, because they show the smallest change in the thickness (thinning) compared to the initial state. It should be noted that the most advantageous option in terms of possible ovality (shape A, θ = 30°) lags behind. However, since these are only slight changes in the order of tenths of a percent, this aspect does not have enough weight in terms of choosing an optimized variant of the tool shape.

6 Conclusions

The article was focused on the design of the pressure die geometry in the rotary draw bending of the tube by an angle of 120° on Wafios RBV 60 ST CNC bending machine. The tube with the diameter of 27 mm and the wall thickness of 3.2 mm was analysed. In this case, the optimisation was performed mainly based on the requirement to reduce ovality with support of the finite element method using the simulation software ANSYS Workbench 2020R2. Firstly, the accuracy of the numerical simulation calculation was verified by comparison with experimental measurements. Subsequently, the effect of the two proposed pressure die geometries was analysed, which replace its initial shape with only two- (shape A) and three-point (shape B) contact between the tube and the tool.

The numerical results of simulations verified the influence of the proposed tools on the resulting ovality and wall thinning of the bend tube for all investigated cases, where tool angle θ varied from 20° to 100°. Based on the simulation results, the final shape of the optimized pressure die groove with angle θ = 30° considering only two point contacts between the formed tube and the die (shape A) was determined, which showed the best results. By optimizing the geometry of the pressure die according to the mentioned parameters, the ovality of the tube at the bending point was improved by an average of 15.5 % (maximal improvement of 21.7 %). However, compared to the initial state, there is a greater thinning of the tube wall, but it is negligible with a value of 0.55 %. Among other things, it has been shown that the optimization makes sense, although it brings an improvement in ovality at the most exposed bending point. Although the article dealt only with the optimization of the pressure die geometry, it was proved that the mentioned optimization makes sense and improves the resulting bend.

Due to other possibilities of optimizing the bending process, in the future, it is planned to assess the influence not only of the pressure die geometry, but also its combination with other parameters, such as bend die geometry, axial compressive force, etc.

Acknowledgement

The paper was supported by project "Analysis of formability and weldability of materials produced by 3D wire metal printing" within the specific research of Faculty of Mechanical Engineering, Brno University of Technology relating to the grant no. FSI-S-20-6336.

References

[1] SAMEK, R., ŠMEHLÍKOVÁ, E., LIDMILA, Z. (2011). *Special Technology of Forming Metals*. CERM, Brno.

[2] PETERKOVÁ, E. (2016). Biaxial test of tubes using elastomer. In: *Manufacturing technology*. Vol. 16, No. 4, pp.765–771. J. E. Purkyne University. Czech Republic.

[3] SAFDARIAN, R. (2019). Investigation of tube fracture in the rotary draw bending process using experimental and numerical methods. In: *Journal of Material Forming*. Vol. 13, No. 4, pp. 493-516. Springer-Verlag, France. ISSN 1960-6206

[4] ŠROM, J. (2017). *Analysis of Tube Bending Process*. Brno University of Technology. Czech Republic.

[5] LIU, Y., DAXIN, E. (2011). Effects of cross-sectional ovalization on springback and strain distribution of Circular tubes under bending. In: *Journal of Materials Engineering and Performance*. Vol. 20, No. 9, pp. 1283-1317. Springer US. Boston. ISSN 1059-9495

[6] MILLER, J. E., KYRIAKIDES, S., BASTARD, A. H. (2001). On bend-stretch forming of aluminum extruded tubes - I: experiments. In: *International Journal of Mechanical Sciences*. Vol. 43, No. 5, pp. 1591-1599. Elsevier. ISSN 0020-7403.

[7] GHAFOOR, K. (2001). How material influences bending for hydroforming: Effects on ovality, springback, and wall thickness in tubes. In: *The Tube & Pipe Journal*. Vol. 4, No. 1, pp. 50-119. Springer-Verlag. New York. ISSN 0162-9700

[8] LI, H., YANG, H., KOU, Y. L. (2010). Deformation behaviors of thin-walled tube in rotary draw bending under push assistant loading conditions. In: *Journal of Materials Processing Technology*. Vol. 210, No. 1, pp. 143-158. Elsevier. ISSN 0924-0136

[9] WEN, T. (2014). On a new concept of rotary draw bend-die adaptablefor bending tubes with multiple outer diameters under non-mandrel condition. In: *Journal of Materials Processing Technology*. Vol. 214, No. 2, pp. 311-317. Elsevier. ISSN 0924-0136

[10] FOREJT, M., JOPEK, M., BUCHAR, J. (2004). Estabilishing the dynamic mechanical properties of materials by the Hopkinson test method. In: *Acta Mechanica Slovaca*. Vol. 8, No. 2B, pp. 93-98. Technical University of Košice. Slovakia. ISSN: 1335- 2393

[11] JOPEK, M. (2021). Determination of Carbon Steel Dynamic Properties. In: *Manufacturing Technology*. Vol. 21, No. 4, pp. 479-482.

[12] KOREČEK, D., SOLFONK, P., SOBOTKA, J. (2020). Numerical Simulation as a Tool to Predict Sheet Metal Forming Process of TRIP Steel HCT690. In: *Manufacturing Technology*. Vol. 20, No. 5, pp.625–631.